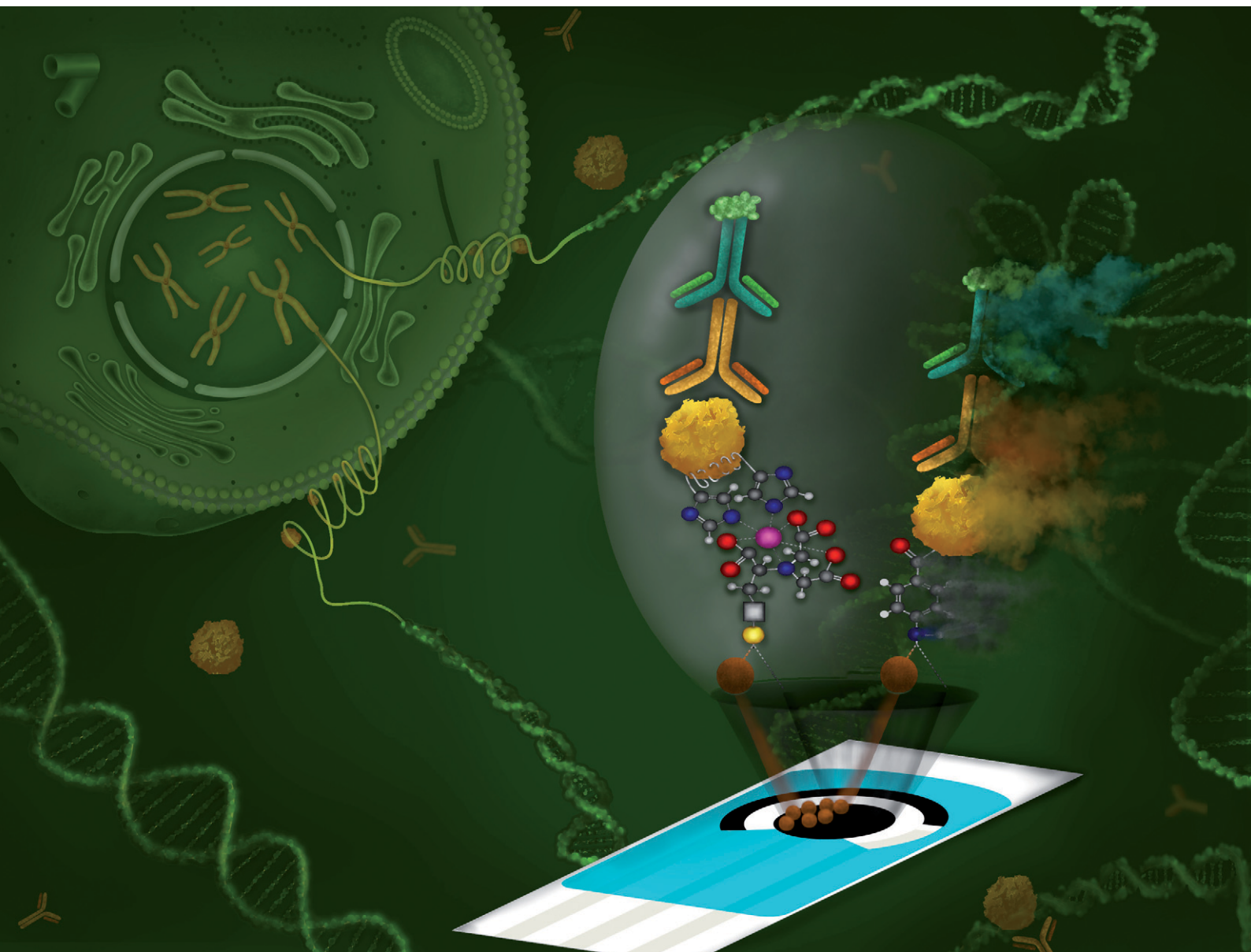


# Sensors & Diagnostics

Volume 2  
Number 2  
March 2023  
Pages 247–470

rsc.li/sensors



ISSN 2635-0998

## COMMUNICATION

Paloma Yáñez-Sedeño, Susana Campuzano,  
José M. Pingarrón *et al.*

First electrochemical bioplatfoms to determine  
anti-centromere B antibodies: critical comparison between  
integrated and magnetic bead-assisted strategies using  
His-tag chemistry



Cite this: *Sens. Diagn.*, 2023, 2, 256

Received 31st October 2022,  
Accepted 21st November 2022

DOI: 10.1039/d2sd00193d

[rsc.li/sensors](https://rsc.li/sensors)

## First electrochemical bioplat­forms to determine anti-centromere B antibodies: critical comparison between integrated and magnetic bead-assisted strategies using His-tag chemistry†

Beatriz Arévalo, Marina Blázquez-García, Alejandro Valverde, Verónica Serafín, Paloma Yáñez-Sedeño, \* Susana Campuzano \* and José M. Pingarrón \*

**This work reports and compares the first electrochemical bioplat­forms for determining anti-centromere B antibodies developed in magnetic microbead-assisted or integrated formats and proves the competitiveness of the nitrilotriacetic acid chemistry they exploit against common carbodiimide/succinimide-based one and their potential to determine serum target autoantibodies at clinically relevant levels.**

The immune system is responsible for protecting the body from potentially harmful substances. Unfortunately, hypersensitivity reactions sometimes occur in which the immune system produces antibodies against the body's own components. These autoantibodies increase the circulating autoreactive cells and favour the development of autoimmune diseases.

Numerous studies have demonstrated the dysregulation of autoantibodies to intracellular components, such as centromeric proteins, which are the basis for the assembly of the kinetochore, a macromolecular complex essential for the precise segregation of chromosomes during mitosis.<sup>1</sup> Anti-centromere antibodies (ACAs), polyclonal autoantibodies directed primarily to three of the centromeric proteins (CENPA, CENPB and CENPC),<sup>2,3</sup> are detected in patients with various autoimmune, rheumatic and cancer diseases.<sup>1</sup> ACAs are considered diagnostic biomarkers in systemic sclerosis (SSc) and are mainly associated with the limited cutaneous subset (LSSc) of this disease which is also known as CREST syndrome. Deregulation of ACAs has also been reported in systemic lupus erythematosus (SLE), primary biliary cholangitis (PBC), rheumatoid arthritis (RA), Sjögren syndrome (SjS) and Raynaud's phenomenon.<sup>1–7</sup>

In particular, the serum level of IgG-type autoantibodies against CENPB, commonly referred to as CENPB-Abs, the main and most clinically relevant ACAs,<sup>1,6,7</sup> is considered as a relevant biomarker for early and minimally invasive diagnosis and follow-up and risk stratification of these diseases.

The detection of the serum level of specific autoantibodies can be performed using indirect immunofluorescence, enzyme linked immunosorbent assay (ELISA), immunodiffusion, line immunoblot assay and light scattering immunoassay.<sup>4–6</sup> Commercial ELISA kits routinely used for these determinations provide adequate sensitivity and selectivity but are poorly compatible with point-of-care (POC) applications. As is known, electroanalytical bioplat­forms are particularly attractive tools for the determination of clinical biomarkers, including specific autoantibodies,<sup>8</sup> because they are easy to use and exhibit short assay times and compatibility with multiplexed and/or multiomics determinations in any environment and by any user. However, to the best of our knowledge, no electroanalytical bioplat­forms have been reported in the literature for the specific determination of CENPB-Abs.

To fill this gap, we report in this work the design, optimization, and application of unique bioplat­forms developed so far for the determination of CENPB-Abs. Two different strategies for the construction of the bioplat­forms were developed and compared. The first strategy is a magnetic microparticle (MB)-based format involving the immobilization of the CENPB protein on a magnetic substrate for the efficient and selective capture of specific autoantibodies (CENPB-Abs) that were enzymatically labelled with a secondary antibody for the most clinically relevant immunoglobulin isotype (IgG) conjugated to the horseradish peroxidase enzyme (HRP-antiIgG). The second strategy involved the immobilization of CENPB onto Co<sup>2+</sup>-tetradentate nitrilotriacetic acid (NTA)-modified screen-printed carbon electrodes (SPCEs) and a similar labelling. In both cases, the

Department of Analytical Chemistry, Faculty of Chemistry, Complutense University of Madrid, 28040, Madrid, Spain. E-mail: [yseo@quim.ucm.es](mailto:yseo@quim.ucm.es), [susanacr@quim.ucm.es](mailto:susanacr@quim.ucm.es), [pingarro@quim.ucm.es](mailto:pingarro@quim.ucm.es)

† Electronic supplementary information (ESI) available. See DOI: <https://doi.org/10.1039/d2sd00193d>



transduction was performed by amperometry at the SPCEs using a  $\text{H}_2\text{O}_2$ /hydroquinone (HQ) system. Unlike electrochemical bioplatfroms recently developed for the determination of particular Abs which exploited the immobilization of target antigens forming amide-<sup>9</sup> or amidine-<sup>10</sup> type covalent bonds, through HaloTag technology<sup>11–14</sup> or streptavidin–biotin affinity reaction,<sup>15,16</sup> or by interacting with the carboxylic acid groups of the polycarbonate used as a separator in arrays of nanoelectrodes,<sup>17,18</sup> the strategies reported in this work used NTA chemistry for the immobilization through the hexahistidine (His) tag expressed in a commercially available CENPB.

Immobilization on NTA *via* a His-tag is considered competitive with covalent immobilization exploiting carbodiimide (EDC)/sulfo-succinimide (Sulfo-NHS) chemistry in terms of simplicity, selectivity, sensitivity, and possibility of regeneration under mild conditions. In addition, the high affinity His-tag immobilization strategy allows working with low concentrations of the immobilized biomolecule, is highly specific because only the His-tagged target protein will be immobilized, avoiding the untagged proteins, and leads to oriented immobilization and adequate spacing, thus avoiding large densities of immobilized biomolecules, which improves the efficiency of the interaction with the solution phase or the solid support.<sup>19,20</sup>

For all these reasons and with the purpose of developing competitive biotools for the determination of CENPB-Abs, in this work, two biosensing platforms for the determination of

CENPB-Abs were developed involving either a MB-assisted or integrated format. The commercially available CENPB with a 6× His-tag at the N-terminus was immobilized through this tag on the surface of MBs suitable for the immobilization of His-tagged proteins (His-tag-isolation-MBs, Fig. 1a), or on the surface of the working electrode of a SPCE modified with NTA and a tetradentate cobalt complex (Fig. 1b). Specific IgG class autoantibodies directed against CENPB were selectively captured on both substrates and enzymatically labelled with a secondary antibody conjugated to the horseradish peroxidase enzyme (HRP-antiIgG) for amperometric detection using a  $\text{H}_2\text{O}_2$ /HQ system, providing a cathodic current variation directly proportional to the concentration of CENPB-Abs.

It is important to mention that although a thiolated long alkyl-NTA derivative was employed for SPCE modification; as reported previously,<sup>21</sup> similar ordered physisorbed layers were formed on these substrates using a non-thiolated analogue, which allows concluding that the thiol moiety did not play an important role in the adsorption of long-chain alkyl-NTA derivatives on the carbon surface. Moreover, it has been reported that this type of compound adsorbs with their long axis parallel to the graphite surface.<sup>22</sup>

Since the objective of this research was, on the one hand to develop competitive bioplatfroms on both supports, and on the other hand to critically compare their performance, we compared them using the optimized experimental conditions for the bioplatfroms prepared on each substrate, which, as expected, were different.

Therefore, studies were carried out to optimize key experimental variables and to demonstrate the reliability of the strategy (control experiments and characterization of the stepwise integrated immunosensing platform fabrication by EIS and CV) and its competitive advantages over other more commonly employed strategies (covalent immobilization with EDC/Sulfo-NHS). The results of all these studies (Fig. S1–S5 and Table S1) and their discussion are given in the ESI†

The analytical and operational characteristics of each bioplatfrom were evaluated and compared. Under the selected working conditions, calibration graphs displayed in Fig. 2 were constructed for the amperometric determination of CENPB-Abs standards. The equation parameters and the analytical features are summarized in Table S2 (in the ESI†).

As can be seen, the immunoplatfrom assisted by MBs achieved a lower LOD (0.006 vs. 0.11  $\text{U mL}^{-1}$ ) and a wider linear range (0.02–200 vs. 0.35–250  $\text{U mL}^{-1}$ ), which is attributed to the larger CENPB loading that can be immobilized as well as the more efficient recognition of the target Abs by improving the binding kinetics by working in suspension under constant stirring.<sup>23–26</sup> It is important to note that the determination of CENPB-Abs using both platfroms can be performed in 45 min. However, counting from the preparation of CENPB-MBs, the construction of the immunoplatfrom takes only 15 min, while the preparation of CENPB- $\text{Co}^{2+}$ -NTA-SPCEs needed 3 h 15 min.

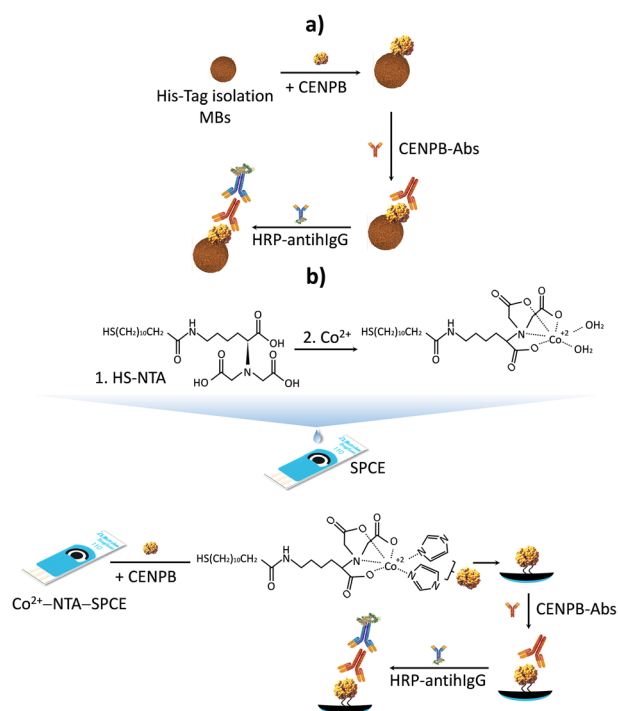


**Fig. 1** Schematic display of the bioplatfroms constructed for the amperometric determination of CENPB-Abs assisted by using MBs a) or an integrated format b).





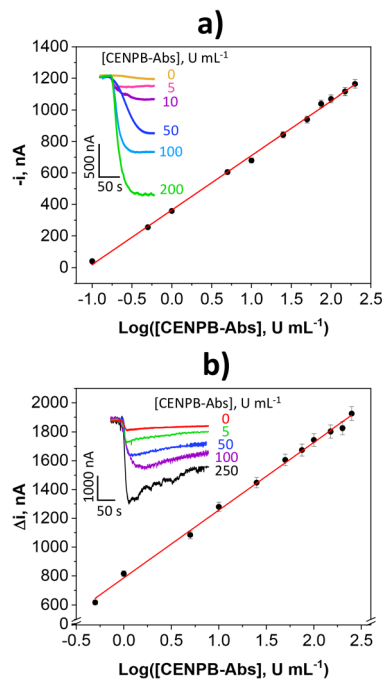


**Fig. 2** Calibration plots and amperometric traces (inset) provided by the MB-assisted a) and integrated b) immunoplateforms for the determination of CENPB-Abs standards.

It should be highlighted that the analytical characteristics achieved with both immunoplateforms are competitive with those claimed for the ELISA methodology. Indeed, in addition to shorter assay times and compatibility of use at the POC, the developed immunoplateforms provided lower LODs since commercially available ELISA kits claim LODs between 0.2 and 10 U mL<sup>-1</sup>.<sup>27–29</sup> Moreover, the linear ranges of the calibration plots extend from concentrations which are clearly below the established CENPB-Abs (IgG) cut-off values in serum to discriminate healthy individuals from patients diagnosed with autoimmune (*e.g.*, 7 U mL<sup>-1</sup> in SSc)<sup>30</sup> and rheumatic (*e.g.*, 10 U mL<sup>-1</sup> in CREST syndrome)<sup>29</sup> diseases.

To evaluate the repeatability of the measurements and the reproducibility of the method, the amperometric responses for 10 U mL<sup>-1</sup> CENPB-Abs standard solutions measured with ten different immunoplateforms prepared in the same manner were recorded. RSD values of 2.3 and 2.5% for measurements made in the same day, and 2.8 and 2.9% in different days, were obtained using the MB-assisted or integrated bioplateforms, respectively. These results show well the good precision and reliability of the manufacturing and electrochemical detection processes involved with both immunoplateforms.

The storage stability of the integrated bioplateforms and the protein-functionalized microparticles was checked. So, different batches of CENPB-MBs and different CENPB-Co<sup>2+</sup>-NTA-SPCEs were prepared on the same day. All were stored at 4 °C, the former resuspended in 50 µL of filtered 10 mM PBS (pH 7.4) in 1.5 mL microcentrifuge tubes, and the latter

stored in a humid chamber. Each control day, the amperometric responses provided by the immunoplateforms prepared from both batches in the absence and presence of CENPB-Abs standards were compared. As Fig. S6 (in the ESI†) shows, the CENPB-MBs can be stored for 30 days and the CENPB-Co<sup>2+</sup>-HS-NTA-SPCEs for 25 days without a significant loss of sensitivity.

In addition to storage stability, the possibility of reusing NTA-modified supports profiting the His-tag chemistry was evaluated. The amperometric responses obtained with the two types of bioplateforms in the absence and in the presence of CENPB-Abs were measured after surface regeneration by incubation for 3 h in a 50 mM phosphate solution (pH 8.0) containing 300 mM NaCl, 300 mM imidazole and 0.01% Tween 20 under continuous stirring and after 40 min in deionized water.<sup>21</sup> This protocol leads to the substitution of the His ligand by imidazole and consequently to the release of immobilized CENPB. Fig. S7 (in the ESI†) shows the amperometric responses obtained when the Co<sup>2+</sup> coordination, CENPB immobilization and CENPB-Abs recognition protocols were repeated on both regenerated substrates. According to the results, both types of substrates can be regenerated at least 5 times, without an apparent loss of sensitivity, indicating the reversibility of the immobilization strategy used as compared to other immobilization methods which, in addition to being more laborious, leads to irreversible anchoring of biomolecules.

The effects of the presence of other antibodies and proteins that can be found in serum, at concentrations reported for healthy individuals, on the response of both immunoplateforms were evaluated. Fig. S8 (in the ESI†) shows that none of the tested substances significantly interfered with the determination of the target autoantibodies when integrated platforms were used. However, the presence of human IgGs showed a noticeable interference with MB-based bioplateforms, which was attributed to their adsorption on the magnetic microsubstrates<sup>15,16</sup> and to the presence of multiple histidines in their Fc region of the immunoglobulins. Fortunately, this interference was minimized if the sample is diluted 100-fold. It is important to note that the higher interference observed for human IgGs when working with the MB-assisted bioplateform compared to the integrated bioplateform should be considered as a particular case, because of the well-documented advantages of MBs for improving selectivity and minimizing sample matrix effects.<sup>23–26</sup>

The practical usefulness of the developed immunoplateforms was tested by analysing serum samples collected from healthy individuals and from subjects considered CENPB-Abs positive.

Previously, the accuracy of the results provided by the bioplateforms was evaluated by analysing the controls (negative and positive) supplied in the centromer B antibody IgG ELISA kit (Cat. no.: DEIA1684) with concentrations of 3 and 35 U mL<sup>-1</sup>, respectively. The results obtained (mean value ± *ts*/√*n*; *n* = 3; α = 0.05) by applying the protocols



described in the Experimental section (in the ESI†) using the MB-assisted and integrated bioplatforms, respectively, were:  $3.1 \pm 0.2$  and  $3.2 \pm 0.2$  U mL<sup>-1</sup> for the negative control and  $35 \pm 2$  and  $34 \pm 2$  U mL<sup>-1</sup> for the positive control, thus confirming the high accuracy of the determinations performed with the immunoplatforms.

In addition, the possible existence of matrix effects in the serum samples was evaluated using serum subjected to different dilution factors. The results obtained showed that samples diluted to 1/50 and 1/1000 did not exhibit matrix effects and the amperometric responses fell within the linear range provided by integrated and MB-assisted immunoplatforms, respectively. Therefore, the concentration of CENPB-Abs was determined by interpolating the amperometric responses provided by the immunoplatforms for the diluted samples into the calibration graphs constructed with standards (Fig. 2).

The obtained results are shown in Fig. 3, while Table S3 (in the ESI†) summarizes such results as well as those obtained with the ELISA methodology. For comparative purposes, the contents that the marketplace (Central BioHub®), from which the CENPB-Abs positive serum samples were purchased, indicated in the specifications are also shown in the table.

As expected, significantly larger CENPB-Abs concentrations were found for individuals classified as positive compared to those for healthy subjects. It is important to highlight that the determined concentrations agreed with the cut-off values established to discriminate healthy individuals from patients positive for this biomarker and diagnosed with autoimmune and rheumatic diseases ( $7\text{--}10$  U mL<sup>-1</sup>).<sup>29–31</sup> Furthermore, the agreement of the concentrations provided by the bioplatforms with those indicated by the online marketplace from which the CENPB-

Abs positive human biospecimens were acquired was excellent.

Moreover, the  $t_{\text{exp}}$  values<sup>32</sup> given in Table S3† were lower in all cases than  $t_{\text{tab}}$  (4.303 at the chosen significance level,  $\alpha = 0.05$ ), and the parameters gathered in the last row of Table S3† coming from the excellent correlations shown on the right side of Fig. 3 confirmed the absence of significant differences between the results provided by the developed bioplatforms and the widely employed ELISA methodology. All these results confirm the accuracy and reliability of the developed immunoplatforms.

The apparatus and electrodes, reagents and solutions and all the procedures used are described in detail in the ESI.†

All experiments were conducted in accordance with institutional guidelines. Furthermore, since all human serum samples tested were purchased from an online marketplace for human biospecimens (Central BioHub®), no informed consents were obtained from the human participants in this study and no ethics committee assurance numbers need to be cited.

This work reports the first electrochemical bioplatforms described to date for the determination of CENPB-Abs. The bioplatforms were implemented on integrated substrates or on the surface of magnetic microparticles. The immunoplatform assisted by MBs provided an 18-fold lower LOD ( $0.006$  vs.  $0.11$  U mL<sup>-1</sup>, both well below the established serum cut-off value of  $7$  U mL<sup>-1</sup> to discriminate between individuals considered positive and negative for CENPB-Abs), and a slightly wider linear range and exhibited a shorter preparation time ( $15$  min vs.  $3$  h  $15$  min). Nevertheless, both immunoplatforms possess analytical and operational characteristics able to fulfil the challenging demands of today's clinic in terms of sensitivity, simplicity, affordability, compatibility with multiplexed or multiomics determinations, and in field operation.

It should be pointed out that the choice between an integrated or MB-assisted bioplatform is neither simple nor universal and must be thoroughly evaluated on a case-by-case basis. Since there is no significant difference between the costs per determination using both bioplatforms (the small amount of MBs and employed immunoreagents limits the cost in both cases compared to that of the SPCE), the selection will be conditioned mainly by the required sensitivity and the composition and viscosity of the sample to be analyzed. For example, for the determination in scarcely diluted serum samples, and due to the discussed IgG interference on magnetic microcarriers, the integrated bioplatforms are probably more attractive. However, in the analysis of saliva samples, with higher viscosity and low IgG content, it would probably be more convenient to use a MB-assisted bioplatform to improve the binding kinetics by working in suspension under constant stirring. It should be also mentioned that, in general, there is a general trend to think that integrated formats (as biosensors used in glucometers) are easier to implement in POCT devices than those based on the use of MBs.

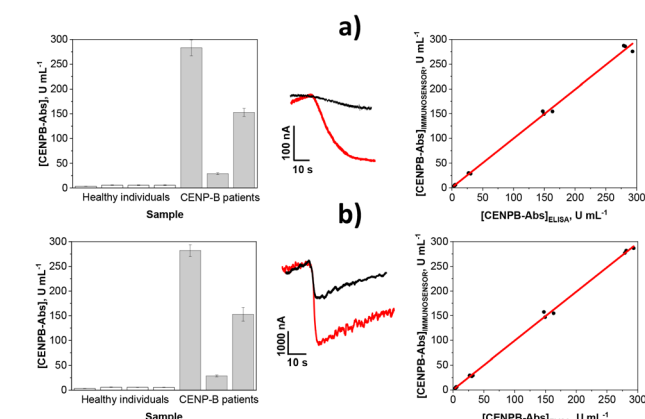


**Fig. 3** Left: CENPB-Abs concentrations provided by the immunoplatforms in serum samples from healthy subjects and CENPB-Abs positive individuals. Centre: Representative amperometric responses recorded for samples from a control subject (in black) and a CENPB-Abs-positive individual (in red). Right: Correlation between the results provided by the developed immunoplatforms and the ELISA methodology. MB-assisted a) and integrated b) immunoplatforms.



The developed bioplatfroms are also attractive compared to the widely accepted ELISA methodology in terms of cost, assay time and applicability in any environment. In terms of applicability, the immunoplatfroms are suitable for the simple, accurate and reliable determination of CENPB-Abs in serum after simple sample dilution which avoids matrix effects. These capabilities may help to deepen the clinical role of this type of biomarker for the early detection and prognosis of diseases of high clinical relevance such as autoimmune and rheumatic disorders and to look for their associations with cancer diseases. The reported results also show that His-tag chemistry provides important advantages over covalent carbodiimide/succinimide immobilization methods, in terms of simplicity, cost, assay time, reusability and sensitivity, for the development of bioplatfroms involving antigen immobilization for the determination of specific autoantibodies.

Beatriz Arévalo: methodology, investigation, and writing – review & editing of original draft. Marina Blázquez-García: methodology and investigation. Alejandro Valverde: methodology and investigation. Verónica Serafín: methodology, investigation, and review & editing of original draft. Paloma Yáñez-Sedeño: conceptualization, supervision, resources, review & editing of original draft, and funding acquisition. Susana Campuzano: conceptualization, supervision, resources, writing, review & editing of original draft, and funding acquisition. José M. Pingarrón: supervision, resources, and review & editing of original draft.

The financial support from RTI2018-096135-B-I00 (Spanish Ministerio de Ciencia, Innovación y Universidades), PID2019-103899RB-I00 (Spanish Ministerio de Ciencia e Innovación) Research Project and the TRANSNANOAVANSENS-CM Program from the Comunidad de Madrid (Grant S2018/NMT-4349) is gratefully acknowledged. B. A. and A. V. acknowledge predoctoral contracts from the Spanish Ministerio de Ciencia, Innovación y Universidades (PRE2019-087596) and Complutense University of Madrid, respectively.

## Conflicts of interest

“There are no conflicts to declare”.

## Notes and references

- 1 R. M. Prasad, A. Bellacosa and T. J. Yen, *J. Mol. Pathol.*, 2021, **2**, 281–295.
- 2 Y. Muro, N. Azuma, H. Onouchi, M. Kunitatsu, Y. Tomita, M. Sasaki and K. Sugimoto, *Clin. Exp. Immunol.*, 2000, **120**(1), 218–223.
- 3 M. Mahler, L. Maes, D. Blockmans, R. Westhovens, X. Bossuyt, G. Riemekasten, S. Schneider, F. Hiepe, A. Swart, I. Gürtler, K. Egerer, M. Fooker and M. J. Fritzler, *Arthritis Res. Ther.*, 2010, **12**(3), R99.
- 4 N. Bizzaro, F. Bonelli, E. Tonutti, D. Villalta and R. Tozzoli, *Clin. Exp. Rheumatol.*, 2002, **20**(1), 45–51.
- 5 T. Dick, R. Mierau, P. Bartz-Bazzanella, M. Alavi, M. Stoyanova-Scholz, J. Kindler and E. Genth, *Ann. Rheum. Dis.*, 2002, **61**(2), 121–127.
- 6 K. Hanke, M. O. Becker, C. S. Brueckner, W. Meyer, A. Janssen, W. Schlumberger, F. Hiepe, G. R. Burmester and G. Riemekasten, *J. Rheumatol.*, 2010, **37**(12), 2548–2552.
- 7 N. Kajio, M. Takeshita, K. Suzuki, Y. Kaneda, H. Yamane, K. Ikeura, H. Sato, S. Kato, H. Shimizu, K. Tsunoda and T. Takeuchi, *Ann. Rheum. Dis.*, 2021, **80**(5), 651–659.
- 8 S. Campuzano, M. Pedrero, A. González-Cortés, P. Yáñez-Sedeño and J. M. Pingarrón, *Anal. Methods*, 2019, **11**, 871–887.
- 9 S. Guerrero, E. Sánchez-Tirado, L. Agüí, A. González-Cortés, P. Yáñez-Sedeño and J. M. Pingarrón, *Talanta*, 2022, **243**, 123304, DOI: [10.1016/j.talanta.2022.123304](https://doi.org/10.1016/j.talanta.2022.123304).
- 10 A. F. Cruz-Pacheco, J. Quinchia and J. Orozco, *Microchim. Acta*, 2022, **189**, 228, DOI: [10.1007/s00604-022-05322-5](https://doi.org/10.1007/s00604-022-05322-5).
- 11 M. Garranzo-Asensio, A. Guzmán-Arangué, C. Povés, M. J. Fernández-Aceñero, R. M. Torrente-Rodríguez, V. Ruiz-Valdepeñas-Montiel, G. Domínguez, M. Villalba, J. M. Pingarrón, S. Campuzano and R. Barderas, *Anal. Chem.*, 2016, **88**, 12339–12345.
- 12 M. Garranzo-Asensio, A. Guzmán-Arangué, E. Povedano, V. Ruiz-Valdepeñas Montiel, C. Povés, M. J. Fernández-Aceñero, A. Montero-Calle, G. Solís-Fernández, S. Fernández-Diez, J. Camps, M. Arenas, N. Cabré, J. Joven, N. Rodríguez, G. Domínguez, P. Yáñez-Sedeño, J. M. Pingarrón, S. Campuzano and R. Barderas, *Theranostics*, 2020, **10**, 3022–3034.
- 13 A. Montero-Calle, I. Aranguren-Abeigón, M. Garranzo-Asensio, A. Guzmán-Arangué, C. Povés, M. J. Fernández-Aceñero, J. Martínez-Useros, R. Sanz, J. Dziaková, J. Rodríguez-Cobos, G. Solís-Fernández, E. Povedano, M. Gamella, R. M. Torrente-Rodríguez, M. Alonso-Navarro, V. de los Ríos, J. I. Casal, G. Domínguez, J. M. Pingarrón, A. Peláez-García, S. Campuzano and R. Barderas, *Engineering*, 2021, **7**, 1393–1412.
- 14 A. Valverde, A. Montero-Calle, B. Arévalo, P. San Segundo-Acosta, V. Serafín, M. Alonso-Navarro, G. Solís-Fernández, J. M. Pingarrón, S. Campuzano and R. Barderas, *Analysis Sensing*, 2021, **1**, 161–165.
- 15 B. Arévalo, V. Serafín, M. Sánchez-Paniagua, A. Montero-Calle, R. Barderas, B. López-Ruiz, S. Campuzano, P. Yáñez-Sedeño and J. M. Pingarrón, *Biosens. Bioelectron.*, 2020, **160**, 112233, DOI: [10.1016/j.bios.2020.112233](https://doi.org/10.1016/j.bios.2020.112233).
- 16 B. Arévalo, M. Blázquez, V. Serafín, A. Montero-Calle, M. Calero, A. Valverde, R. Barderas, S. Campuzano, P. Yáñez-Sedeño and J. M. Pingarrón, *Bioelectrochemistry*, 2022, **144**, 108041, DOI: [10.1016/j.bioelechem.2021.108041](https://doi.org/10.1016/j.bioelechem.2021.108041).
- 17 H. B. Habtamu, M. Sentic, M. Silvestrini, L. De Leo, T. Not, S. Arbault, D. Manojlovic, N. Sojic and P. Ugo, *Anal. Chem.*, 2015, **87**, 12080–12087.
- 18 H. B. Habtamu, T. Not, L. De Leo, S. Longo, L. M. Moretto and P. Ugo, *Sensors*, 2019, **19**, 1233, DOI: [10.3390/s19051233](https://doi.org/10.3390/s19051233).
- 19 L.-J. Zhou, R.-F. Li, X.-Y. Li and Y.-W. Zhang, *Eng. Life Sci.*, 2021, **21**, 364–373.



- 20 C. Ley, D. Holtmann, K.-M. Mangold and J. Schrader, *Colloids Surf., B*, 2011, **88**, 539–551.
- 21 F. Conzuelo, M. Gamella, S. Campuzano, P. Martínez-Ruiz, M. Esteban-Torres, B. de las Rivas, A. J. Reviejo, R. Muñoz and J. M. Pingarrón, *Anal. Chem.*, 2013, **85**, 3246–3254.
- 22 T. Bhinde, S. M. Clarke, T. K. Phillips, T. Arnold and J. E. Parker, *Langmuir*, 2010, **26**, 8201–8206.
- 23 T. A. P. Rocha-Santos, *TrAC, Trends Anal. Chem.*, 2014, **62**, 28–36.
- 24 L. Reverte, B. Prieto-Simon and M. Campas, *Anal. Chim. Acta*, 2016, **908**, 8–21.
- 25 J. Kudr, B. Klejdus, V. Adam and O. Zitka, *TrAC, Trends Anal. Chem.*, 2018, **98**, 104–113.
- 26 M. Pastucha, Z. Farka, K. Lacina, Z. Mikusova and P. Skladal, *Microchim. Acta*, 2019, **186**, 312, DOI: [10.1007/s00604-019-3410-0](https://doi.org/10.1007/s00604-019-3410-0).
- 27 [https://steffens-biotech.com/wp-content/uploads/2020/03/CENP-B\\_igG\\_1511FE00.FWD\\_.pdf](https://steffens-biotech.com/wp-content/uploads/2020/03/CENP-B_igG_1511FE00.FWD_.pdf).
- 28 [https://shop.tinyteria.com/index.php?route=extension/module/free\\_downloads/download&did=675](https://shop.tinyteria.com/index.php?route=extension/module/free_downloads/download&did=675).
- 29 [https://products.orgentec.com/pdfs/ifu/ORG%20633\\_IFU\\_EN\\_QM113209\\_2018-01-02\\_3.pdf](https://products.orgentec.com/pdfs/ifu/ORG%20633_IFU_EN_QM113209_2018-01-02_3.pdf).
- 30 N. M. van Leeuwen, M. Boonstra, J. A. Bakker, A. Grummels, S. Jordan, S. Liem, O. Distler, A. M. Hoffmann-Vold, K. Melsens, V. Smith, M. E. Truchetet, H. U. Scherer, R. Toes, T. W. J. Huizinga and J. K. de Vries-Bouwstra, *Arthritis Rheumatol.*, 2021, **73**(12), 2338–2347.
- 31 <https://www.thermofisher.com/phadia/es/es/product-catalog.html?articleNumber=14-5505-01&region=ES>.
- 32 J. N. Miller and J. C. Miller, *Statistics and Chemometrics for Analytical Chemistry*, Pearson Education Limited, 6th edn, 2010, ISBN-10: 0273730428.

